Truncated Moments of the F_2 Structure Function for Barely Offshell Neutrons

BONUS Collaboration

(Dated: July 21, 2014)

PACS numbers:

Keywords:

I. INTRODUCTION

Inclusive electron scattering has proven a reliable way of probing nuclear and nucleon structure. In particular the structure functions of the nucleon extracted from inclusive scattering experiments exhibit several of the key features of Quantum Chromodynamics (QCD): quark confinement at large distance scale and asymptotic freedom at the short distance (high energy) scale.

Since the late 1960s this type of experiment has yielded an impressive body of data mapping the proton structure functions over several orders of magnitude in the scaling Bjorken variable x and the squared four momentum transfer variable Q^2. These data provided strong constraints on the quark and gluon momentum distributions (PDFs) of the nucleon. In order to unambiguously extract the individual PDFs and $d(x)$ in particular, one needs structure function data on the neutron as well. The absence of a high density free neutron target has hampered these efforts. Most experiments obtain neutron data by separately extracting the structure function for hydrogen and light nuclei (deuterium, helium) and then subtracting the (smeared) proton result from the nuclear result [1–4].

A phenomenon called quark–hadron duality has rather surprisingly shown [5, 6] to link the high and low momentum and mass regions of measured F_2 data. In a QCD framework quark–hadron duality can be explained via the Operator Product Expansion (OPE) [7]. At fixed x and for large Q^2 the structure function moments can be expressed as an inverse power series of Q^2. This expansion allows the separation between the non–perturbative contributions contained in the parton correlation functions (lower momentum, resonance mass region) from the "hard" scattering of the probe from partons in the high momentum, mass region. Testing quark–hadron duality for the neutron has been difficult due to the lack of a neutron target.

Availability of extensive and precise structure function data in wide range of x and Q^2 has led to in–depth studies of the quark–hadron duality phenomenon. This phenomenon was first observed by Bloom and Gilman [8] in 1970 and in essence states that the structure function measured in the resonance region mimics on average the deep inelastic scattering result. This behavior, first documented for the F_2 proton structure function, was recently observed for other observables [9–11].

A relatively new approach in the study of quark–hadron duality is the use of "truncated" structure function moments [12]. In analogy with "full" moments of the F_2 structure function "truncated" moments are defined as:

$$M_n(x_{min}, x_{max}, Q^2) = \int_{x_{min}}^{x_{max}} dx x^{n-2} F_2(x, Q^2), \tag{1}$$

where the integration over x is restricted to an interval (x_{min}, x_{max}). This method avoids extrapolation of the integrand into poorly mapped kinematic regions, and is particularly well suited for the study of local duality where an x region can be defined by a resonance mass width.

The current paper presents a study of local quark–hadron duality for the neutron using free neutron structure function data obtained at Jefferson Lab using the novel BONuS detector and CLAS spectrometer. Four ranges in the invariant mass squared W^2 corresponding to the three prominent resonance regions ($1.3 \le W^2 \le 1.9$ GeV^2 for the first resonance region, $1.9 \le W^2 \le 2.5$ GeV^2 for the second resonance region, and $2.5 \le W^2 \le 3.1$ GeV^2 for the third resonance region) plus the whole resonance region ($1.3 \le W^2 \le 4.0$ GeV^2) were selected. While a similar study based on a model–dependent extraction of F_2^n exists [2], the results reported here are the first from an experimentally–isolated neutron target, and hence have significantly smaller (theoretical) systematic uncertainties.

II. THE BONUS EXPERIMENT

The results reported here rely on a novel experimental technique aimed at eliminating or at least reducing some of the theoretical uncertainties involved in the subtraction procedure described above. The BONuS (Barely Off–shell Nucleon Structure) experiment [13–15] used a Radial Time Projection Chamber (RTPC) to tag backward–moving, low momentum spectator protons in conjunction with the CLAS detector [16] in experimental Hall B at Jefferson Lab to study electron scattering off of a gas deuteron target. By tagging low momentum backward moving spectator protons one minimizes final state interactions [17–19] and places the neutron just barely off–shell [14]. Additionally, Fermi smearing effects are essentially eliminated.

The BONuS experiment ran in 2005 and acquired electron–deuteron scattering data at three electron beam energies: 2.140, 4.223, and 5.262 GeV. In order to isolate electron–neutron interactions this experiment used an RTPC based on three layers of gas electron multipliers surrounding a thin, pressurized gas deuterium target to tag spectator protons with momenta as low as 70 MeV/c. The scattered electron was detected by CLAS, a hermetic spectrometer installed in the experimental Hall B. The experiment and data analysis are described in detail in [15]. Ratios of neutron to proton F_2 structure functions and neutron F_2 structure function were extracted over a wide range of kinematic values and for proton spectator momenta between 70 and 100 MeV/c. The total systematic uncertainty in the neutron structure function extracted is 8.7% [15]. Additionally there is an overall 10% scale uncertainty due to cross normalization of the BONuS data to existing F_2^n/F_2^d parameterizations.

The kinematic coverage shown in Figure 1 (4.223 and 5.262 GeV results combined) extends from the quasielastic peak to the deep inelastic region corresponding to final state hadron masses of ~ 3 GeV. The curves shown represent the W^2 thresholds for the regions mentioned above. Typical F_2^n results for $Q^2 = 1.2$ and $Q^2 = 2.4$ GeV^2 are shown in Figure 2. The open/closed symbols correspond to 4.2 and 5.2 GeV electron beam energies respectively. Predictions, with and without higher twist effects, of the QCD fit ABKM [20] are also shown. It should be noted that the data

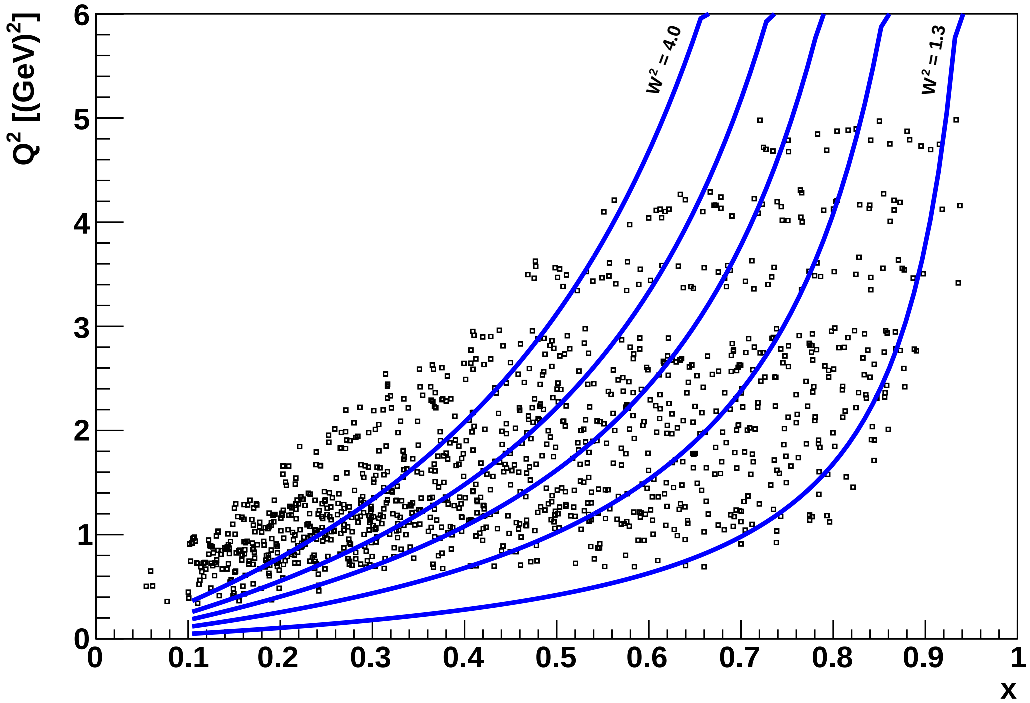

FIG. 1: Kinematic coverage of the BONuS data. The lines represent the W^2 thresholds for the four regions mentioned in the text.

used in this analysis were obtained for backward–moving (angles between proton spectator and the momentum transfer vector larger than 100°) low spectator proton momenta (less than 100 MeV) thus minimizing the effects of final state interaction and off–shell effects.

III. TRUNCATED MOMENTS AND LOCAL QUARK–HADRON DUALITY

As Q^2, x, and W^2 are not independent of each other, a range in W^2 at fixed Q^2 implies a corresponding range in x. This allows for a straightforward integration of the experimental F_2^n

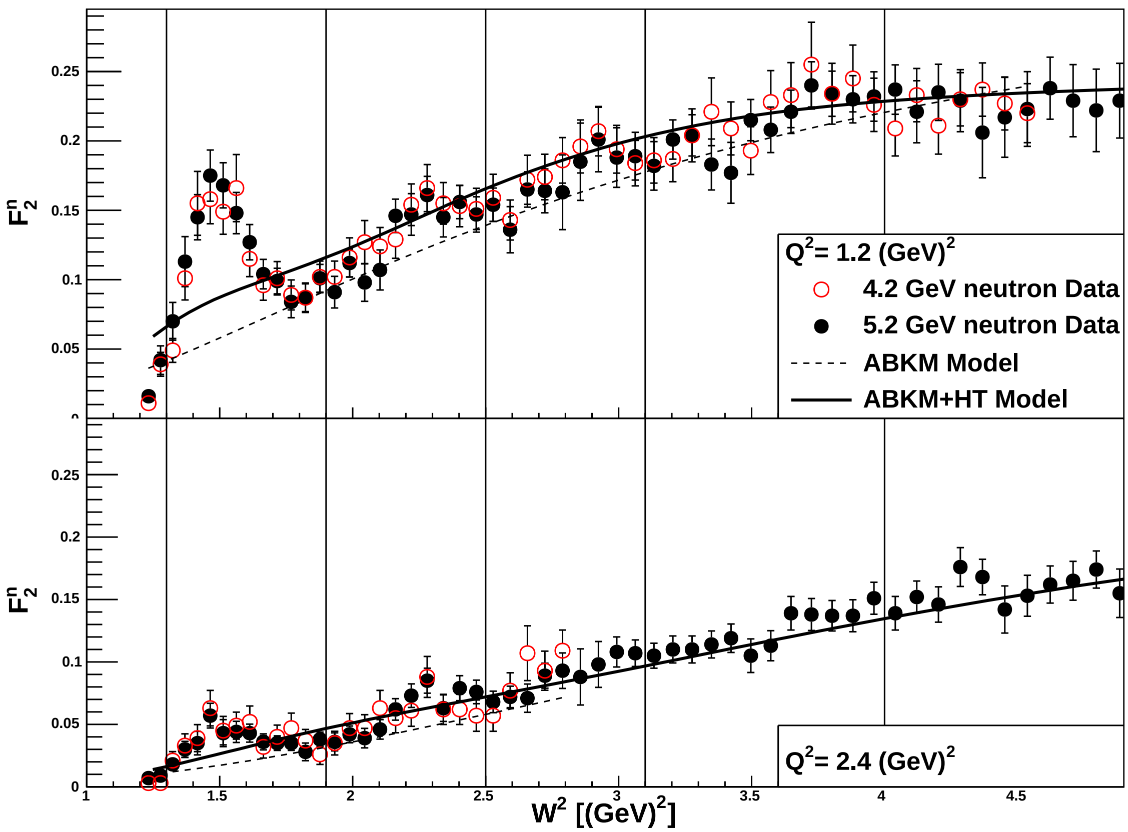

FIG. 2: Typical neutron structure function data from the BONuS experiment at $Q^2 = 1.2$ GeV^2 (top panel) and $Q^2 = 2.4$ GeV^2 (bottom panel). The open circles represent data obtained with a beam energy of $E = 4.2$ GeV, while the closed circles were obtained with $E = 5.2$ GeV beam energy. The curves shown are the ABKM DIS parameterizations [20] with (solid line) and without (dashed line) higher twist effects.

structure function data to obtain truncated moments. In order to minimize model dependence, the integrals were evaluated based solely on the experimentally measured points without using any inter- or extrapolating function. The second ($n = 2$) truncated moments, M_2 obtained from these data are shown in Fig. 3 as a function of Q^2, and are listed in Table I. The uncertainties quoted take into account the experimental statistical and systematic uncertainties and include a 10%

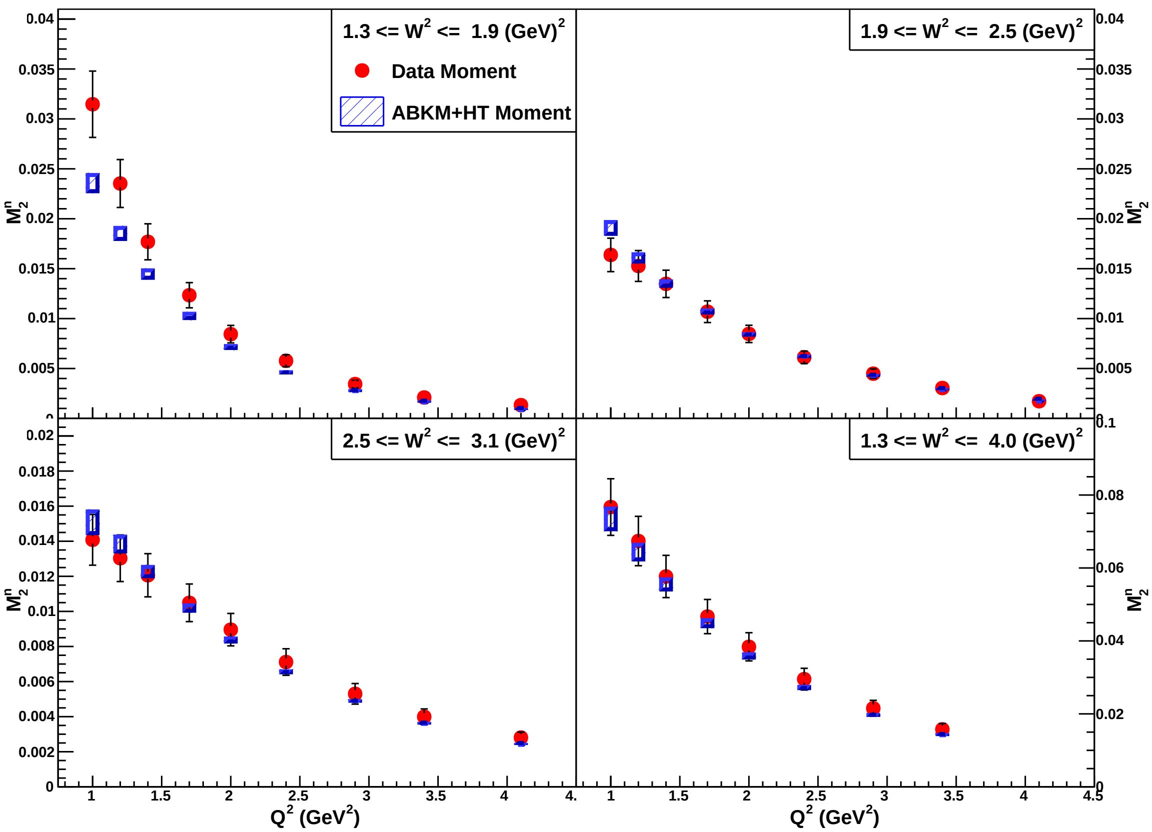

FIG. 3: The neutron truncated moments as a function of Q^2. The closed circles represent the moments obtained from the BONuS data, while the blue rectangles are the moments obtained from the ABKM parameterization [20] which includes target mass and higher twist corrections.

scale/normalization uncertainty for all points. The corresponding higher order truncated moments ($n = 4$ and $n = 6$) are shown in Tables II and III, respectively.

In order to study local duality we formed the ratio of the truncated moments of F_2^n in the resonance region obtained from the BONuS data to the neutron moments calculated over the same x range based on the ABKM QCD fit [20]. These results are shown as a function of Q^2 in Fig. 4 (closed circles) for M_2. For the M_2 moments the earlier, model–dependent results from [2] are also shown

Q^2	$1.3 \leq W^2 \leq 1.9$	$1.9 \leq W^2 \leq 2.5$	$2.5 \leq W^2 \leq 3.1$	$1.3 \leq W^2 \leq 4.0$
1.00	3.147e-02 $\pm$ 3.3e-03	1.638e-02 $\pm$ 1.7e-03	1.408e-02 $\pm$ 1.4e-03	7.670e-02 $\pm$ 7.8e-03
1.20	2.353e-02 $\pm$ 2.4e-03	1.527e-02 $\pm$ 1.5e-03	1.303e-02 $\pm$ 1.3e-03	6.739e-02 $\pm$ 6.8e-03
1.40	1.769e-02 $\pm$ 1.8e-03	1.348e-02 $\pm$ 1.4e-03	1.206e-02 $\pm$ 1.2e-03	5.767e-02 $\pm$ 5.8e-03
1.70	1.234e-02 $\pm$ 1.3e-03	1.069e-02 $\pm$ 1.1e-03	1.049e-02 $\pm$ 1.1e-03	4.668e-02 $\pm$ 4.7e-03
2.00	8.440e-03 $\pm$ 8.8e-04	8.466e-03 $\pm$ 8.6e-04	8.959e-03 $\pm$ 9.2e-04	3.839e-02 $\pm$ 3.9e-03
2.40	5.774e-03 $\pm$ 6.0e-04	6.123e-03 $\pm$ 6.3e-04	7.114e-03 $\pm$ 7.6e-04	2.952e-02 $\pm$ 3.0e-03
2.90	3.441e-03 $\pm$ 3.7e-04	4.484e-03 $\pm$ 4.7e-04	5.302e-03 $\pm$ 5.9e-04	2.153e-02 $\pm$ 2.2e-03
3.40	2.096e-03 $\pm$ 2.5e-04	3.047e-03 $\pm$ 3.3e-04	3.994e-03 $\pm$ 4.5e-04	1.575e-02 $\pm$ 1.6e-03
4.10	1.331e-03 $\pm$ 1.7e-04	1.723e-03 $\pm$ 2.1e-04	2.809e-03 $\pm$ 3.1e-04	N/A

TABLE I: Second order truncated moments of the neutron F_2 structure function based on the BONuS data for the four W^2 regions studied.

(open circles). The four panels correspond to the four invariant mass regions previously defined. The computed ABKM moments include higher twist effects and target mass corrections. The figure also presents the ratio of truncated F_2 neutron moments computed using the CTEQ–Jlab (CJ) parameterization [21] with respect to the same ABKM moments.

To study the influence of target mass corrections and higher twists the CJ model was used to obtain both the leading twist (thin dashed line) and the higher twist (thick solid line) predictions. The latter also included target mass corrections. The differences between the two models presented are within the uncertainty of the data. Taking into account that, in the resonance region, target mass corrections and higher twist effects are expected to be sizable the comparison of the data moments to leading twist parameterization predictions is rather poor. Models that include HT and TMC effects produce a data–to–theory ratio much closer to unity, especially in the second and third resonance region.

As seen in Fig. 4, in the first W range, data moments are 20–40% larger than the model expectation. While the BONuS results reported here are in good agreement with the earlier findings based

Q^2	$1.3 \leq W^2 \leq 1.9$	$1.9 \leq W^2 \leq 2.5$	$2.5 \leq W^2 \leq 3.1$	$1.3 \leq W^2 \leq 4.0$
1.00	1.158e-02 ± 1.2e-03	3.091e-03 ± 3.2e-04	1.687e-03 ± 1.7e-04	1.749e-02 ± 1.8e-03
1.20	9.803e-03 ± 1.0e-03	3.505e-03 ± 3.6e-04	1.950e-03 ± 2.0e-04	1.678e-02 ± 1.7e-03
1.40	8.106e-03 ± 8.3e-04	3.604e-03 ± 3.7e-04	2.169e-03 ± 2.2e-04	1.561e-02 ± 1.6e-03
1.70	6.272e-03 ± 6.4e-04	3.396e-03 ± 3.5e-04	2.326e-03 ± 2.4e-04	1.401e-02 ± 1.4e-03
2.00	4.673e-03 ± 4.9e-04	3.076e-03 ± 3.1e-04	2.356e-03 ± 2.4e-04	1.245e-02 ± 1.3e-03
2.40	3.483e-03 ± 3.7e-04	2.542e-03 ± 2.6e-04	2.198e-03 ± 2.3e-04	1.059e-02 ± 1.1e-03
2.90	2.224e-03 ± 2.4e-04	2.109e-03 ± 2.2e-04	1.933e-03 ± 2.1e-04	8.524e-03 ± 8.7e-04
3.40	1.436e-03 ± 1.7e-04	1.578e-03 ± 1.7e-04	1.638e-03 ± 1.8e-04	6.723e-03 ± 6.9e-04
4.10	9.524e-04 ± 1.3e-04	9.805e-04 ± 1.2e-04	1.292e-03 ± 1.4e-04	N/A

TABLE II: Fourth order truncated moments of the neutron F_2 structure function based on the BONuS data for the four W^2 regions studied.

on the proton subtraction technique (open circles) [2], and both are consistent with unity in the second and third resonance region, they are consistently higher in the first resonance region. It should be noted that while all local duality studies on the neutron are sensitive to binding effects, Fermi motion, and final state interactions, obtaining neutron structure functions by subtracting (smeared) proton from deuteron data is especially sensitive to the nuclear models employed at the largest x (i.e. smallest W) values. This increases the dependence and possibly bias of the subtraction method result on various theoretical assumptions and models [3].

Interestingly, in all cases, the moments of the resonance region display the same Q^2 dependence (i.e. a flat Q^2 dependence in Fig. 4) as the PDF–based parameterizations. This is a remarkable confirmation of one aspect of duality, i.e. that the bound, large x and lower Q, region can nonetheless be described by the same evolution and correction equations– displaying the same dynamics– as the higher Q, larger W, scattering regime of single quark deep inelastic scattering. This is true even for the very largest x, lowest W, area. Here, the uncertainties on the PDFs are large and could easily account for the $\sim 20\%$ strength difference, but not the Q^2–dependence.

Q^2	$1.3 \leq W^2 \leq 1.9$	$1.9 \leq W^2 \leq 2.5$	$2.5 \leq W^2 \leq 3.1$	$1.3 \leq W^2 \leq 4.0$
1.00	4.391e-03 ± 4.7e-04	5.959e-04 ± 6.1e-05	2.048e-04 ± 2.1e-05	5.279e-03 ± 5.6e-04
1.20	4.188e-03 ± 4.3e-04	8.192e-04 ± 8.3e-05	2.953e-04 ± 3.0e-05	5.454e-03 ± 5.5e-04
1.40	3.794e-03 ± 3.9e-04	9.782e-04 ± 9.9e-05	3.941e-04 ± 4.0e-05	5.375e-03 ± 5.4e-04
1.70	3.241e-03 ± 3.3e-04	1.092e-03 ± 1.1e-04	5.203e-04 ± 5.3e-05	5.167e-03 ± 5.2e-04
2.00	2.621e-03 ± 2.7e-04	1.129e-03 ± 1.2e-04	6.239e-04 ± 6.4e-05	4.819e-03 ± 4.9e-04
2.40	2.122e-03 ± 2.2e-04	1.063e-03 ± 1.1e-04	6.834e-04 ± 7.2e-05	4.409e-03 ± 4.5e-04
2.90	1.449e-03 ± 1.6e-04	9.982e-04 ± 1.1e-04	7.082e-04 ± 7.8e-05	3.774e-03 ± 3.9e-04
3.40	9.893e-04 ± 1.2e-04	8.216e-04 ± 9.0e-05	6.741e-04 ± 7.5e-05	3.140e-03 ± 3.3e-04
4.10	6.846e-04 ± 9.2e-05	5.605e-04 ± 6.8e-05	5.962e-04 ± 6.6e-05	N/A

TABLE III: Sixth order truncated moments of the neutron F_2 structure function based on the BONuS data for the four W^2 regions studied.

Local quark–hadron duality in the proton F_2 structure function has been studied extensively [5, 6], showing possible violations mainly in the first resonance region, although these are potential violations of the total integral and not the critically important comparison of Q^2 dependence. To compare the proton with the neutron results, similar ratios of truncated moments (resonance/deep inelastic region) were constructed for the proton using the ABKM model to calculate the deep inelastic moment and a global fit [22] for the resonance region. This ratio is shown in Fig. 4 as open squares. It can be seen that, with the exception of the first resonance region, the ratios for proton and neutron are very similar and indicate that quark–hadron duality holds locally for both nucleons. In the first resonance region however, there are sizable (15% or more) deviations from the total, but not the Q^2 trend both for proton and the neutron. It is interesting to note that for the proton the resonance region falls systematically below one, while for the neutron this ratio is consistently above one. This can be indicative of a fundamental difference between the proton and the neutron at the very largest x values. Alternatively, this can be the result of the fact that QCD fits for either proton or neutron are not well constrained at large x, which is the kinematic range of the first resonance

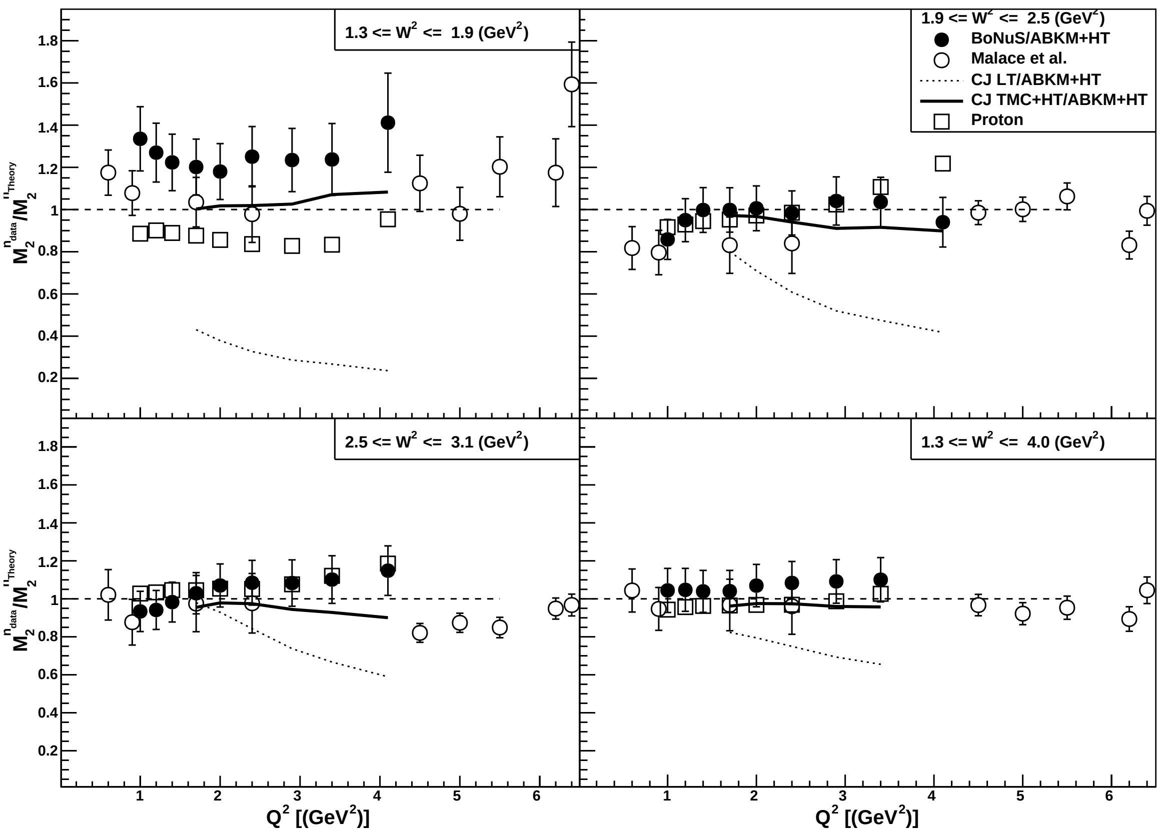

FIG. 4: The ratios of M_2 truncated moments for the neutron structure function F_2 and the proton (closed circles) obtained from the BONuS data. The open circles represent the model–dependent results obtained by [2]. The open squares represent the same ratio of truncated moments for the proton. The lines represent comparisons of the ABKM with the CJ model: thick solid line for the case when TMC and HT effects are included in both models, thin dashed line when the CJ model is evaluated only for leading twist.

region.

Fig. 5 shows the ratio of the neutron–to–proton truncated moments (closed circles) as a function of Q^2 for the four resonance regions. The proton moments were evaluated for the exact BONuS kinematics using the phenomenological model [22]. The line shown is the ratio of neutron and proton

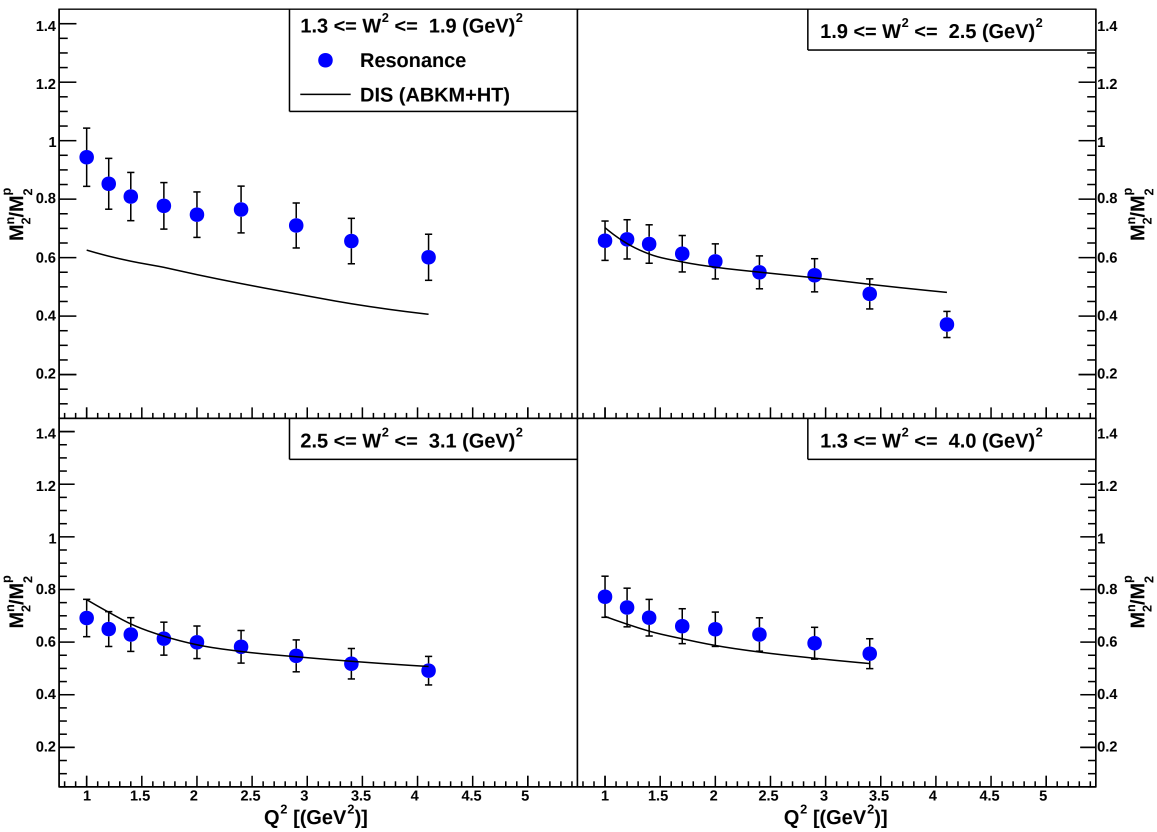

FIG. 5: The ratio of neutron to proton F_2 truncated moments, M_2 for the four regions studied. The closed circles represent the BONuS results, while the solid line corresponds to the ABKM QCD fit prediction including HT and TMC.

truncated moments calculated using the ABKM (including HT and TMC) model. The model agrees well with the data in the second and third resonance regions but it substantially underestimates the data in the first resonance region. In conventional parameterizations of parton distribution functions the d/u ratio tends to either zero or infinity as $x \to 1$, depending on the parameterization of the d PDF [23]. At x above 0.8 the uncertainties on the PDFs, especially the d, are considerable, due to deuteron nuclear model corrections and to the lack of high x data. Predictions of F_2^n/F_2^p vary in the

0.25 to 0.5 range, with higher values possible depending on the nuclear corrections used [23]. Based on SU(6) symmetry and quark model predictions one expects equal excitation strengths for both Δ^0 and Δ^+, which would imply a F_2^n/F_2^p ratio of one. Therefore violations of local quark hadron duality are expected to be greatest in this region. This is consistent with the results reported here which indicate that close to $Q^2 = 0$ limit the data tends toward unity, then slowly decreasing as the photon virtuality increases.

The data presented here enable the extension of the isospin dependence of duality in the second and third resonance regions. Assuming, as some quark models do [24–26], a dominance of magnetic couplings the proton resonance data should overestimate the DIS prediction in these regions due to the odd–parity resonances, such as the prominent spin$-1/2$ octet, resulting in a measured neutron–to–proton truncated moment ratio that should fall below the corresponding DIS curve. As shown in Fig. 5 the results presented here do not support this argument.

IV. CONCLUSION

In conclusion, this paper investigated local quark–hadron duality in the neutron structure function based on data obtained by the BONuS experiment at Jefferson Lab using a novel experimental technique to tag the spectator proton in a deuterium target. This technique provides smaller systematic uncertainties than earlier studies that relied on the subtraction of smeared hydrogen data from deuterium. Truncated F_2 structure function moments were compared to PDF fits based on deep inelastic scattering data, as well as to similar truncated moments obtained for the proton. The results indicate that quark–hadron duality holds dynamically everywhere, as well as in sum for the second and third resonance regions. The advantages of the spectator tagging technique and the higher energy beam that will become available at Jefferson Lab will allow for more detailed studies of quark hadron duality and neutron structure in the future.

---

[1] O. Hen, E. Piasetzky, L.B. Weinstein, D.W. Higinbotham, JLAB–PHY–11–1440, arXiv:1109.6197.

[2] S.P. Malace, Y. Kahn, W. Melnitchouk,C.E. Keppel, Phys. Rev. Lett. **104**, 102001 (2010).

[3] J. Arrington, J.G. Rubin, W. Melnitchouk, Phys. Rev. Lett. **108**, 252001 (2012)

[4] M. Osipenko, W. Melnitchouk, S. Simula, S. Kulagin, G. Ricco, Nucl. Phys. **A766**, 142 (2006).

[5] S.P. Malace *et al.*, Phys. Rev. C **80**, 035207 (2009).

[6] I. Niculescu *et al.*, Phys. Rev. Lett. **85**, 1186 (2000).

[7] A. DeRujula, H. Georgi, H.D. Politzer, Ann. Phys. **103**, 315 (1975).

[8] E.D. Bloom and F.G. Gilman, Phys. Rev. Lett. **25**, 1140 (1970).

[9] P. Solvignon *et al.*, Phys. Rev. Lett. **101**, 182502 (2008).

[10] P. Bosted *et al.*, Phys. Rev. **C75**, 035203 (2007).

[11] W. Melnitchouk, R. Ent, C.E. Keppel, Phys. Rep. **406**, 127 (2005).

[12] A. Psaker, W. Melnitchouk, M.E. Christy, C. Keppel, Phys. Rev. **C78** 025206 (2008).

[13] H. Fenker *et al.*, Nucl. Instr. Meth. **A592**, 273 (2008).

[14] N. Baillie *et al.*, Phys. Rev. Lett. **108**, 199902 (2012).

[15] S. Tkachenko *et al.*, Phys. Rev. **C89**, 045206 (2014).

[16] B.A. Mecking *et al.*, Nucl. Instr. Meth. **A503**, 513 (2003).

[17] C. Ciofi degli Atti, L.P. Kaptari, B.Z. Kopeliovich, Eur. Phys. J. A **19**, 133 (2004).

[18] W. Cosyn and M. Sargsian, Phys. Rev. **C84**, 014601 (2011).

[19] W. Cosyn, W. Melnitchouk, and M. Sargsian, Phys. Rev. **C89**, 014612 (2014).

[20] S. Alekhin, J. Blumlein, S. Klein, S. Moch, Phys. Rev. **D81** 014032 (2010).

[21] A. Accardi *et al.*, Phys. Rev. **D84**, 014008 (2011).

[22] M.E. Christy and P.E. Bosted, Phys. Rev. C **81**, 055213 (2010).

[23] A. Accardi *et al.*, Phys. Rev. **D84**, 014008 (2011).

[24] F. E. Close and N. Isgur, Phys. Lett **B509**, 81 (2001).

[25] F. E. Close and W. Melnitchouk, Phys. Rev. **C68**, 035210 (2003).

[26] F. E. Close and W. Melnitchouk, Phys. Rev. **C79**, 055202 (2009).